RSC Advances

ROYAL SOCIETY OF CHEMISTRY

www.rsc.org/advances

Cite this: DOI: 10.1039/c0xx00000x

www.rsc.org/xxxxxx

ARTICLE TYPE

Large–scale synthesis and characterization of magnetic poly(acrylic acid) nanogels *via* miniemulsion polymerization

Jianan Zhang*, Zhengquan Lu, Mingyuan Wu, Qingyun Wu, Jianjun Yang

Received (in XXX, XXX) Xth XXXXXXXXX 20XX, Accepted Xth XXXXXXXXX 20XX

DOI: 10.1039/b000000x

This article provides a facile method for the large−scale preparation of magnetic poly(acrylic acid) (PAA) nanogels. Cross–linked polyacrylonitrile (PAN) nanoparticles were synthesized via miniemulsion polymerization method using acrylonitrile (AN) and divinyl benzene (DVB) as raw material, and then PAA nanogels were obtained from the cross–linked PAN nanoparticles under the basic conditions. The structure and morphologies of PAN nanoparticles, PAA nanogels, and magnetic PAA nanogels were characterized by Fourier−transformed infrared spectroscopy (FTIR), transmission electron microscopy (TEM), and dynamic light scattering equipment (DLS), respectively. The pH−responsive property of PAA nanogels was investigated by measuring their swelling−deswelling behavior under different pH buffer solutions. The results showed that the obtained PAN nanoparticles were of uniform spherical morphology with wrinkled surface and had a narrow size distribution with an average size of 105 nm in diameter. PAA nanogels were regular spherical particles with an average particle size of 230 nm in diameter. The PAA nanogels demonstrated excellent pH–responsive properties in different pH buffer solutions. After the addition of γ– (trimethoxysilyl) propyl methacrylate (MPS) modified magnetic nanoparticles, magnetic PAA microgels were fabricated successfully.

Introduction

Polymer nanogels are particles in which polymer molecules are cross−linked by chemical or physical bonds.[1] Stimuli−responsive nanogels undergo abrupt changes in volume in response to external stimuli, such as temperature,[2] pH,[3] ionic strength,[4] and changes in solvent composition,[5] which have promising applications in drug release tissue engineering, biosensors, catalytic carriers, optical and chemical separation.[6,7]

Polyacrylic acid (PAA) nanogels have good biocompatibility, and fast responsive property, and a large specific surface area, and remain one of the most ideal candidates in the above applications. Because acrylic acid is water-soluble monomer of high reaction activity and PAA is soluble in polar solvent, it is hard to prepare PAA nanogels directly by conventional emulsion polymerization and solution polymerization method. An alternative methodology is involved using inverse emulsion polymerization or inverse suspension polymerization.8 However, this will introduce large quantity of organic solvent as continuous phase. El-Rehim[9] fabricated PAA nanogels by gamma radiation-induced polymerization of acrylic acid (AAc) in an aqueous solution of polyvinylpyrrolidone (PVP) as a template polymer, but this method required γ-rays generated from a ^{60}Co source and was conducted at a low concentration in the dilute solution (total concentration of 1.5%), resulting in very low yields of nanogels. Es−haghi prepared cross−linked PAA nanogels by precipitation polymerization using an organic solvent as a dispersion medium, but the use of organic solvents brings many restrictions for the real−life applications of the as−fabricated nanogels.[8] Therefore, the large−scale and facile preparation of PAA nanogels still remains to be solved.

Recently, miniemulsion polymerization followed the droplet nucleation mechanism and has been proven to be a versatile way to the morphology controlled preparation of hybrid polymer nanoparticles.[10] Due to the high water solubility of acrylonitrile, the water–phase nucleation of acrylonitrile in miniemulsion polymerization will lead to secondary nucleation. The main obstacle to produce highly uniform PAN nanoparticles based on miniemulsion polymerization is to suppress or eliminate the water–phase nucleation of acrylonitrile.

Based on our previous research,[11−13] we investigated the feasibility of fabrication of magnetic PAA nanogels via miniemulsion polymerization by incorporation of Fe_3O_4 nanoparticles. Herein we report the fabrication of polyacrylonitrile (PAN) nanoparticles via miniemulsion polymerization and the formation of PAA nanogels from the hydrolysis reactions of PAN nanoparticles. By using sodium nitrite ($NaNO_2$) as an aqueous-phase inhibitor, droplet nucleation is dominant in the case of the miniemulsion polymerizations. The morphology and pH−responsive

behavior of PAA nanogels were investigated. This method provides a facile way to the large-scale preparation of magnetic PAA nanogels.

Experimental

Raw materials

Acrylonitrile (AN) and divinyl benzene (DVB) were purchased from Shanghai Chem. Reagent Co. (China) and were purified by passing through a short basic Al_2O_3 column before use. 2, 2`–azobis (isobutyronitrile) (AIBN, Fluka) was purified by recrystallization in absolute ethanol and kept refrigerated until use. γ– (Trimethoxysilyl) propyl methacrylate (MPS, Aldrich) and hexadecane (HD, Fluka) were used without purification. Cetyltrimethylammonium bromide (CTAB), sodium dodecyl sulfate (SDS), $FeCl_2 \cdot 4H_2O$, $FeCl_3 \cdot 6H_2O$, sodium nitrite ($NaNO_2$), and triethylamine (TEA) were purchased from Shanghai Chemical Reagent Co. in their reagent grade and used without further purification. Deionized water was used for all purposes.

Synthesis of MPS modified magnetic (MPS-Fe_3O_4) nanoparticles

The magnetic nanoparticles were prepared by co-precipitation of $FeCl_2/FeCl_3$ (ratio 1:2). An aqueous solution (150 mL) containing 5.6 mM $FeCl_2$ and 11.2 mM $FeCl_3$ in a 250-mL flask was heated to 50 °C under N_2 bubbling. Then 12.5 mL ammonia solution was added under vigorous stirring. After 30 min, the precipitate was collected by a magnet and washed three times with water. Then the precipitate was re-dispersed in ethanol (150 mL) and a certain amount of MPS was added as the surface modifier. The dark suspension was stirred for 8 h at room temperature under N_2 atmosphere. The black precipitate was collected, washed three times with ethanol, and then dried under vacuum at 30 °C overnight.

Synthesis of magnetic PAA nanogels

In a typical synthesis, 0.8 g of HD and 0.3 g of AIBN were first added in the monomer mixtures of 15.0 g of AN, 1.8 g of DVB, and 1.50 g of MPS modified magnetic nanoparticles to form an oil phase. A portion of CTAB aqueous solution was employed as a water phase. The mixture of oil phase and water phase was first pre-emulsified by mechanical stirring for 0.5 h and then the miniemulsion was prepared by Ultra-Turrax®T18 homogenizer (IKA®, Germany) at 19, 000 rpm for 5 min in an ice bath and the polymerization was carried out at 65 °C in a 250-ml four−neck round flask equipped with a reflux condenser and an agitator. After the polymerization was carried out for 8 h under N_2 atmosphere, the pH value of the dispersion was adjusted to around 9.0 by adding NaOH solution. The hydrolysis reactions of cross−linked PAN nanoparticles continued for 5 h at 80 °C to obtain magnetic PAA microgels. The yields of PAN nanoparticles and PAA nanogels were determined by gravimetric analysis. The detailed recipes were listed in Table 1.

Table 1 Synthesis conditions of PAN nanoparticles

Samples	Oil phase					Water phase		
	AN	DVB (g)	HD (g)	AIBN (g)	MPS-Fe_3O_4 (g)	Water (g)	CTAB (g)	SDS (g)
1	15.0	1.20	0.80	0.30	0	80	0.30	0
2	15.0	1.20	0.80	0.30	0	80	0	0.30
3	15.0	1.20	0.80	0.30	0	80	0.20	0.20
4	15.0	0.00	0.80	0.30	0	80	0.50	0
5	15.0	0.60	0.80	0.30	0	80	0.50	0
6	15.0	0.90	0.80	0.30	0	80	0.50	0
7	15.0	1.20	0.80	0.30	0	80	0.50	0
8	15.0	1.50	0.80	0.30	0	80	0.50	0
9	15.0	1.80	0.80	0.30	0	80	0.50	0
10	15.0	1.80	0.80	0.30	0.50	80	0.50	0
11	15.0	1.80	0.80	0.30	1.00	80	0.50	0
12	15.0	1.80	0.80	0.30	1.50	80	0.50	0

0.2 g of $NaNO_2$ was added in water phase using as an aqueous-phase inhibitor.

Characterization

Samples of transmission electron microscopy (TEM) were prepared by drying a drop of dilute nanocomposite dispersion onto a carbon–coated copper grid. Analysis was conducted using a JEM–2100 (JEOL, Japan) electron microscope operating at 200 kV. The average size and size distribution of polymer nanoparticles were determined using light scattering equipment (Zetasizer 3000 HSA, Malvern Company). The samples were previously diluted in water without filtration. Samples of FTIR characterization were dried at 60 °C under vacuum for 24 h and measured in the wavenumber range from 4000 to 400 cm^{-1} at a resolution of 4 cm^{-1} using a Nicolet Nexus–870 FTIR spectrophotometer. The powder X–ray diffraction (XRD) was performed on Rigaku Geigerflex diffractometer with CuKα radiation (λ = 0.15418 nm), and the 2θ angle varied from 16° to 80° at a scanning rate of 2°/min. The vibrating–sample magnetometer (VSM, BHV-55) was used to study the magnetic properties of magnetic nanoparticles.

Results and discussion

The formation mechanism of magnetic PAA nanogels by miniemulsion polymerization

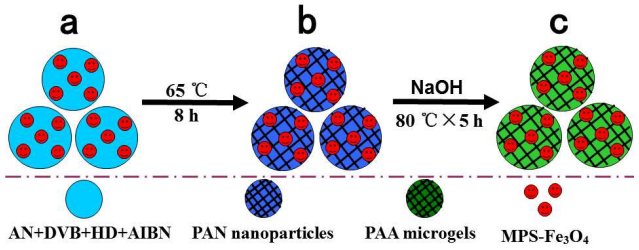

Scheme 1 Illustration for the preparation of magnetic PAA nanogels *via* miniemulsion polymerization.

The fabrication of magnetic PAA nanogels *via* in situ miniemulsion polymerization was displayed in Scheme 1. First of all, the mixture of AN, DVB, MPS-Fe_3O_4 nanoparticles, and HD was restricted in miniemulsion droplets as nanoreactors via miniemulsification process (Scheme 1a). The oil droplets were stabilized by CTAB and HD (Scheme 1a).[12] Due to a small amount of sodium nitrite ($NaNO_2$) solution was added to the miniemulsion, the formation of PAN nanoparticle occured primarily via monomer droplet nucleation. After the polymerization of monomers, cross−linked PAN nanoparticles were obtained (Scheme 1b). When NaOH solution was added, large amounts of hydroxyl ions penetrated into the interior of PAN nanoparticles. PAA nanogels were fabricated successfully after the hydrolysis reactions of PAN (Scheme 1c).

Characterization of magnetic nanoparticles

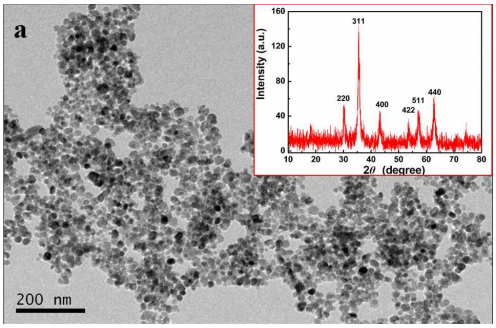

Fig. 1 TEM image of magnetic nanoparticles. Inset shows the XRD pattern of magnetic nanoparticles.

In order to encapsulate magnetic nanoparticles, the as-prepared magnetic nanoparticles should be hydrophobically modified before adding to organic monomers. Fig. 1 shows the TEM image of MPS modified magnetic nanoparticles. As Fig. 1 displays, Fe_3O_4 particles were nearly monodispersed with a size of about 15 nm. Due to the modification by MPS, the hydrophobic magnetic nanoparticles remained well dispersed in organic monomers without agglomeration. The typical XRD pattern of magnetic nanoparticles was shown in the inset of Fig. 1. The exhibited peaks at 2θ angles of 18.3°, 30.2°, 35.5°, 43.2°, 53.6°, 57.2°, 63.0°, and 74.3°, which are consistent with the standard data for magnetite (JCPDS card no. 87-2334). The calculated diameter of magnetite nanoparticles from XRD pattern is about 12 nm by Scherrer's formula,[14] which is consistent with the size observed in TEM image (Fig. 1).

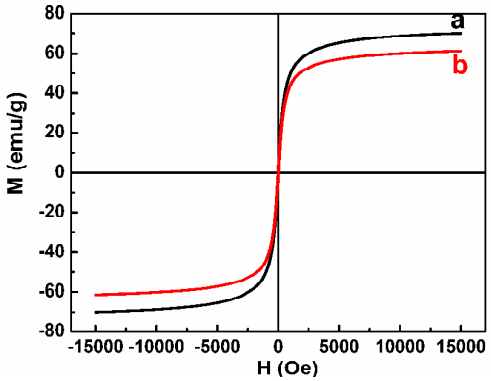

Fig. 2 Magnetization curves of Fe_3O_4 nanoparticles (a) and MPS-Fe_3O_4 nanoparticles (b).

The magnetic properties of Fe_3O_4 nanoparticles and MPS-Fe_3O_4 nanoparticles were analyzed by vibrating sample magnetometer (VSM). The magnetization curve can be obtained by plotting the magnetization of the sample with the applied magnetic field. The saturation magnetization values of magnetic nanoparticles and MPS modified magnetic nanoparticles were about 70.0 emu/g and 61.2 emu/g at 300 K, respectively, as shown in Fig. 2. After surface-modification, the saturation magnetization of MPS-Fe_3O_4 nanoparticles decreased a little because of the existence of MPS on the surface of Fe_3O_4 nanoparticles.[15] Both of these nanoparticles exhibited a clear magnetic response and could readily collected under an external magnetic field.

FTIR analysis of polymer nanoparticles

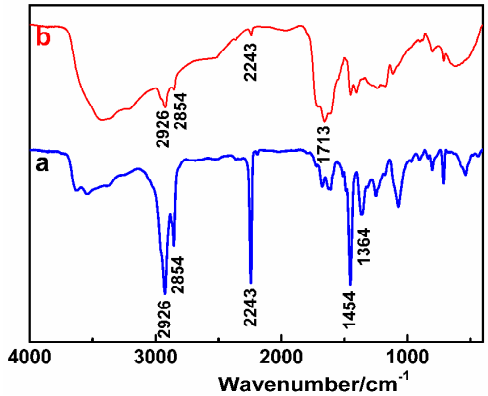

Fig. 3 FTIR spectra of PAN nanoparticles (a) and PAA nanogels (b).

Fig. 3a shows the FTIR spectrum of PAN nanoparticles. The peaks at wavenumber near to 2926 cm^{-1} and 2854 cm^{-1} correspond to the stretching vibration of C−H. The peaks at 1454 cm^{-1} and 1364 cm^{-1} were for the bending vibration absorption of C−H. The band around 2260−2240 cm^{-1} is associated with the characteristic absorption peak of −CN groups. Compared with standard spectra of PAN, the result indicated the successful synthesis of PAN polymer. After hydrolysis reactions of PAN nanoparticles under base conditions, the functional −CN groups were converted to −COOH groups. As can be seen from Fig. 3b, the peak at 2243 cm^{-1} disappeared. Furthermore, the peak appearing at 1713 cm^{-1} is assigned to the stretching vibration absorption of carboxylic carbonyl group (C=O) and the existing O−H

groups in the −COOH groups resulted in the broad peak of stretching vibration absorption at 3000−3300 cm^{-1}. These results confirmed the formation of PAA nanogels after hydrolysis reactions of PAN nanoparticles.[16]

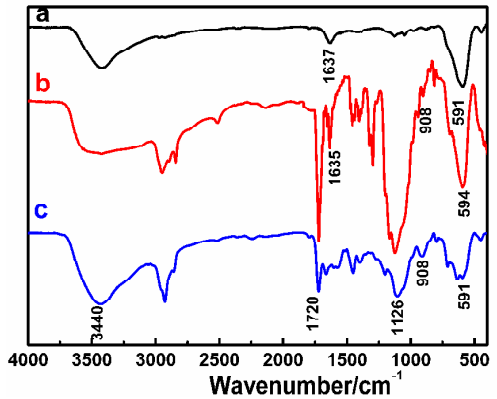

Fig. 4 FTIR spectra of Fe_3O_4 nanoparticles (a), MPS-Fe_3O_4 nanoparticles (b) and Fe_3O_4/PAA hybrid microgels (c).

Fig. 4 shows FTIR spectra of Fe_3O_4 nanoparticles MPS-Fe_3O_4 nanoparticles and Fe_3O_4/PAA hybrid microgels. As can be seen from Fig. 4a, 4b and 4c, the peaks at wavenumber near to 591 cm^{-1} correspond to the stretching vibration absorption of Fe−O. Due to the adsorption amount of −OH on Fe_3O_4 surface, so strong absorption peak appeared in about 3400 cm^{-1}. The peaks at 1720 cm^{-1} and 1637 cm^{-1} were for the characteristic absorption of C=O and C=C groups of MPS in Fig. 4b. The peaks located at 1126 cm^{-1} in Fig. 4b and 4c correspond to the vibration absorption peak of Si−O, which also demonstrated the successful modification of Fe_3O_4 nanoparticles by MPS. The characteristic peak of −CN in the 2243 cm^{-1} disappeared in Fig. 4c, indicating that the complete hydrolysis reactions of PAN nanoparticles. Because the copolymerzaiton of monomers and MPS on magnetic nanoparticles, the absorption peak of C=C at 1637 cm^{-1} became very weak.

The morphologies of PAN nanoparticles and PAA nanogels

Firstly, the influence of the emulsifier content and cross-linking agent on the morphology of composite PAN nanoparticles were investigated. When CTAB was replaced by SDS, agglomerations or sediments were detectable during polymerization process and the as-obtained nanoparticles were polydisperse in particle size (Fig. S1, Fig. S2, see Supporting Materials).

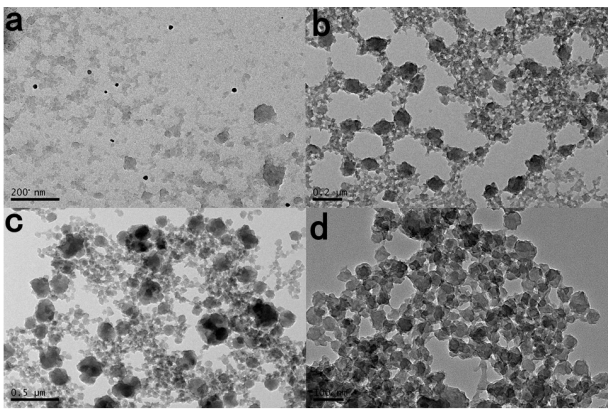

Fig. 5 TEM images of PAN nanoparticles prepared with 0.6 g (a), 0.9 g (b), 1.2 g (c), and 1.5 g (d) of DVB.

For a comparison, different contents of DVB were added in the synthesis of PAN nanoparticles to give various cross-linking density of cross-linked PAN nanoparticles. Without the addition of DVB, large aggregations were found during the polymerization process and the obtained latexes consisted of nanoparticles with the size of 20−30 nm. Because AN monomer has a relatively high solubility in water (7 g/100 mL, 20 °C) , the monomer in the miniemulsion monomer droplets will migrate into water phase and polymerize. The micelle nucleation will dominate. When DVB was added in the oil phase, the polymerization rate will increase greatly and the migration of monmer from droplets would be compressed leading to the donimation of droplet neucleation. As displayed in Fig. 5, when the content of DVB was 0.6 g, only a few nanoparticles can be found in the latexes (Fig. 5a). With the content of DVB increasing from 0.9 g, 1.2 g, to 1.5 g, the spherical morphology of PAN nanoparticles increased gradually (Fig. 5b−d). When the content of DVB increased up to 1.8 g, the obtained PAN nanoparticles had a uniform morphology when 1.8 g of DVB was added (Fig. 6a). Therefore, CTAB was chosen as the emulsifier and the optimal content of DVB determined was 12 wt% of monomers.

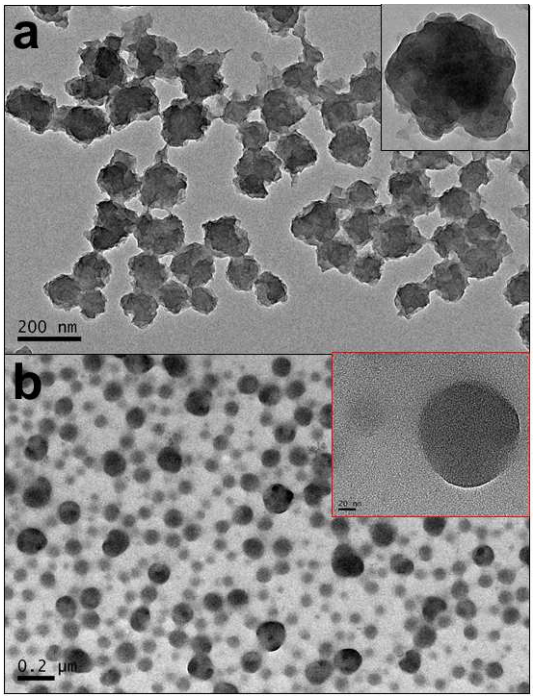

Fig. 6 TEM images of PAN nanoparticles prepared with 1.8 g of DVB (a) and PAA nanogels (b). Insets show the corresponding high-resolution TEM image.

The typical TEM images of PAN nanoparticles and corresponding PAA nanogels were shown in Fig. 6a and Fig. 6b, respectively. As can be seen from Fig. 6a, PAN nanoparticles have a uniform size of about 100 nm before hydrolysis reactions. From the inset of Fig. 6a, we can observe that PAN nanoparticles did not have smooth surface, but showed an irregular spherical structure. This wrinkled surface of PAN nanoparticles also had

been observed by Landfester.[17] Because PAN was not soluble in acrylonitrile monomer, the polymerized acrylonitrile precipitated within the new–forming nanoparticles and led to phase separation during miniemulsion polymerization. In addition to this specific characteristic of PAN polymer, the crystalline properties of PAN resulted in the formation of wrinkled surface PAN nanoparticles. After hydrolysis reactions of PAN nanoparticles, the hydrophobic −CN groups were converted to hydrophilic −COOH groups. Generally PAA nanogels became hydrated and swollen by the absorption and entrance of water, and thus the average size of final nanogels would increased. However, PAA nanogels shunk a little and the size of nanogels remained below 100 nm under TEM determination condition, which can be seen from Fig. 6b.

Size analysis of PAN nanoparticles and PAA nanogels

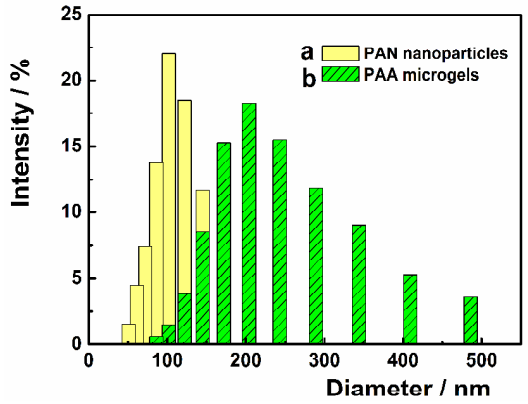

Fig. 7 Size distributions of PAN nanoparticles and PAA nanogels.

Fig. 7 shows the particle size distributions of PAN nanoparticles and PAA nanogels. As can be seen from Fig. 7, both the particle size and size distribution of PAA nanogels had an obvious change after the hydrolysis reactions. The average size of PAN nanoparticles is about 105 nm and had a narrow size distribution. When the original hydrophilic −CN groups of PAN nanoparticles were converted into a hydrophilic −COOH groups, PAA nanogels were obtained. Due to the swelling of PAA nanogels in aqueous solution, the average diameter of PAA nanogels increased to about 230 nm and also the size distribution became broader, which were much larger than that determined by TEM.

pH−responsive behavior of PAA nanogels

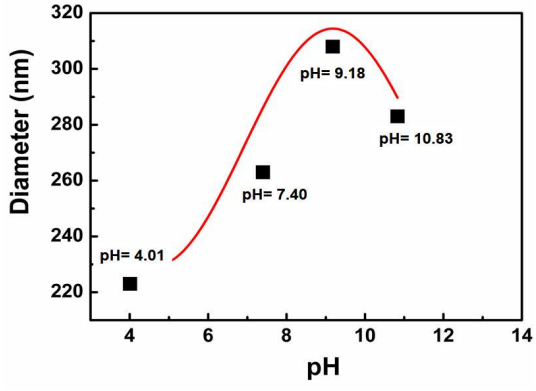

Fig. 8 pH–responsive property of PAA nanogels at pH (a) 4.01, (b) 7.40, (c) 9.18, and (d) 10.83, respectively.

The pH–responsive property of PAA nanogels was investigated by using dynamic light scattering equipment. The particle size distributions of PAA nanogels at different pH buffer solution were shown in Fig. S4. Fig. 8 shows pH responsive property of PAA nanogels. With the increase of pH value, the average particle size of PAA nanogels increased from 223 nm at pH=4.01, 260 nm at pH=7.40, to 308 nm at pH=9.18. PAA nanogels are composed of cross−linked PAA macromolecular chains, which contain a large amount of −COOH groups in their backbones. Because the carboxyl groups were deprotonated at a low pH value (4.01), the negative charge of PAA nanogels reduced and electrostatic repulsion decreased accordingly, which led to the shrinkage of PAA nanogels (Fig. S4a). When the pH value of buffer solution increased to 7.40 and 9.18, −COOH groups were ionized and electrostatic repulsion between macromolecular chains enhanced. This expansion of three−dimensional network structure of cross−linked nanogels gradually led to the significant increase of nanogels size from 223 nm (Fig. S4b) to 308 nm (Fig. S4c). However, when pH value continued to increase up to 10.83, the −COOH groups of PAA had been completely dissociated and the electrostatic repulsion did not increase accordingly. Because the concentration of external ions gradually achieved dynamic Donnan equilibrium, a large number of hydroxyl groups of PAA nanogels produced strong electrostatic shielding effects.[16] This resulted in the gradual contraction of nanogels, and the average size of nanogels reduced from 308 nm to 283 nm (Fig. S4d).

Morphology and properties of magnetic PAA microgels

In order to obtain magnetic PAA microgels, magnetic nanoparticles were modified by MPS and added in the oil phase before the miniemulsification process. After the polymerization of monomers was completed, hydrophobic magnetic nanoparticles should be encapsulated within PAN nanoparticles. As shown in Fig. 9, the obtained magnetic microgels with a size of ~500 nm were prepared successfully by the addition of hydrophobic magnetic nanoparticles in oil phase. The size of magnetic microgels became larger than that prepared without the addition of magnetic nanoparticles. Magnetic hybrid PAA microgels exhibited a clear magnetic response, and could readily be moved and collected with an external magnetic field, which is displayed in the inset of Fig. 9.

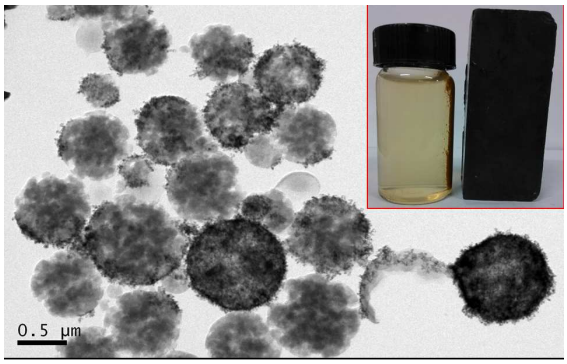

Fig. 9 TEM images of magnetic PAA microgels prepared with the weight ratio of AN/DVB/MPS-Fe_3O_4/HD = 15.0/1.8/1.5/0.80 (Sample 12 in Table 1). Photo of the magnetic microgels under magnetic field was

shown in inset.

The magnetic properties of Fe_3O_4@PAN hybrid nanoparticles and Fe_3O_4@PAA magnetic microgels were analyzed by VSM method. After the encapsulation of MPS-Fe_3O_4 nanoparticles, the saturation magnetization values of magnetic PAN microparticles and PAA microgels decreased greatly to 21.63 emu/g and 19.29 emu/g at 300 K, respectively, as shown in Figure 10a and 10b.

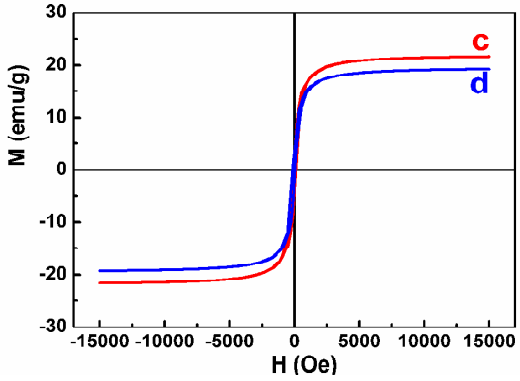

Fig. 10 Magnetization curves of Fe_3O_4@PAN hybrid nanoparticles (a) and Fe_3O_4@PAA hybrid microgels (b).

The incorporation of magnetic nanoparticles in microgels makes it easier to separate drug-loaded microgels with the help of external applied magnetic fields. Furthermore, the magnetic microgels have the properties of targeting transport and controlled release of drugs when combined with their pH-responsive properties microgels.[18] The application of magnetic PAA microgels in controlled release field are being carried out in our laboratory.

Conclusions

To conclude, cross–linked PAN nanoparticles were prepared *via* miniemulsion polymerzation and PAA nanogels were fabricated successfully by hydrolysis recations under base conditions. The obtained PAN nanoparticles of uniform size were about 105 nm in diameter and the particle size of PAA nanogels were about 230 nm. These PAA nanogels showed good pH–responsive property. By adding MPS modified magnetic nanoparticles in oil phase, magnetic PAA microgels are obtained with magnetic nanoparticles embedded in polymeric core, which would have promising applications in biological engineering, drug delivery, chemical separation, and so on.

Acknowledgements

This work was supported by the Doctoral Scientific Research Startup Fund of Anhui University (No. 33190129), the Anhui Provincial Natural Science Foundation (No. 1408085MKL19), and the National Natural Science Foundation of China (No. 21044006 and 51173001).

Notes and references

School of Chemistry and Chemical Engineering, Anhui University and Anhui Province Key Laboratory of Environment–friendly Polymer Materials, Hefei 230601, P. R. China.

E-mail: jiananz1@andrew.cmu.edu

Tel: +86 551 63861745; Fax: +86 551 63861745

1 B. R. Saunders and B. Vincent, *Adv. Colloid Interface Sci.*, 1999, **80**, 1.
2 T. Hoare and R. Pelton, *Macromolecules*, 2004, **37**, 2544.
3 H. Bysell, A. Schmidtchen and M. Malmsten, *Biomacromolecules*, 2009, 10, 2162.
4 S. Neyret and B. Vincent, *Polymer*, 1997, **38**, 6129.
5 A. Pich, Y. Lu, V. Boyko, S. Richter, K.F. Arndt and H. J. P. Adler, *Polymer*, 2004, **45**, 1079.
6 J. K. Oh, R. Drumright, D. J. Siegwart and K. Matyjaszewski, *Prog. Polym. Sci.*, 2008, **33**, 448.
7 L. P. Jiang and P. Liu, *Ind. Eng. Chem. Res.*, 2014, **53**, 2924.
8 H. Es-haghi, H. Bouhendi, G. Bagheri-Marandi, M.J. Zohurian-Mehr and K. Kabiry, *Polym-Plast. Technol.*, 2010, **49**, 1257.
9 H. A. A. El-Rehim, E. S. A. Hegazy, A. A. Hamed and A. E. Swilem, *Eur. Polym. J.*, 2013, **49**, 601
10 K. Landfester, *Angew. Chem. Int. Ed.*, 2009, **48**, 4488.
11 J. A. Zhang, J. J. Yang, Q. Y. Wu, M. Y. Wu, N. N. Liu, Z. L. Jin and Y. F. Wang, *Macromolecules*, 2010, **43**, 1188.
12 J. A. Zhang, S. L. Qiu, Y. L. Zhu, Z. Q. Huang, B. B. Yang, W. L. Yang and J. J. Yang, *Polym. Chem.*, 2013, **4**, 1459.
13 J. A. Zhang, Q. Liu, B. B. Yang, W. L. Yang, B. Wu, J. Z. Lin and J. J. Yang, *Polym. Chem.*, 2012, **3**, 2720.
14 V. S. Zaitsev, D. S. Filimonov, I. A. Presnyakov, R. J. Gambino and B. Chu, *J. Colloid Interface Sci.*, 1999, **212**, 49.
15 I. Prigogine and S. A. Rice, *Adv. Chem. Phys.*, John Willey & Sona, Inc. 1997; Vol. 98.
16 H. Hu, H. Wang and Q. Du, *Soft Matter*, 2012, **8**, 6816.
17 K. Landfester and M. Antonietti, *Macromol. Rapid Commun.*, 2000, **21**, 820.
18 A. P. Esser-Kahn, S. A. Odom, N. R. Sottos, S. R. White and J. S. Moore, *Macromolecules*, 2011, **44**, 5539.